

1 **Priors for natural image statistics inform confidence in perceptual decisions**

2 Rebecca K West^{1*}, Emily J A-Izzeddin², William J Harrison^{1,2}

3 ¹ School of Psychology, University of Queensland, Australia

4 ² Queensland Brain Institute, University of Queensland, Australia

5 * Corresponding author: rebecca.west1@uq.net.au

6

7 Competing Interests: The authors have no competing interests to declare.

8

9 Acknowledgements: We thank Cheyanne Gu for assistance with data collection. This
10 work was funded by an ARC DECRA to WJH (DE190100136).

11

Abstract

12 Decision confidence plays a critical role in humans' ability to make adaptive decisions
13 in a noisy perceptual world. Despite its importance, there is currently little consensus
14 about the computations underlying confidence judgements in perceptual decisions.
15 One leading theory suggests that confidence is computed following the rules of
16 Bayesian inference. Accordingly, the goal of the current study was to investigate a
17 fundamental assumption of Bayesian models: the use of prior knowledge in subjective
18 confidence. Rather than requiring participants to internalise the parameters of an
19 arbitrary prior distribution, we capitalised on the existing probability distributions of
20 features in natural scenes, which are known to play a critical role in guiding perception.
21 Participants reported the subjective upright of naturalistic image target patches, and
22 then reported their confidence in their orientation responses. We used computational
23 modelling to relate the statistics of the targets to participants' responses, confirming
24 that participants used the prior probability distribution of features in natural scenes to
25 judge subjective upright. Critically, our results reveal that participants also used natural
26 image priors to inform their confidence judgements. Our findings provide important
27 evidence supporting a Bayesian characterisation of confidence and highlight the
28 influence of environmental priors on confidence.

29

Introduction

30

31

32

33

34

35

36

37

38

39

40

41

42

43

44

45

Humans make hundreds of decisions about their perceptual world every day and these decisions are often accompanied by a sense of confidence. Confidence can be defined as the belief that a choice or proposition is correct based on the available evidence (Pouget et al., 2016). In a perceptual world where the ‘available evidence’ is often corrupted with noise, confidence judgements play a crucial role in peoples’ ability to make adaptive decisions in the absence of explicit feedback. For example, confidence has been shown to inform subsequent decisions (van den Berg, Zylberberg, et al., 2016) and to guide further information seeking before committing to a choice (Desender et al., 2018). Despite being a salient property of human decision-making, there is currently little consensus about how humans compute their confidence. A prominent theory suggests that confidence is computed following the rules of Bayesian inference (Adler & Ma, 2018; Aitchison et al., 2015; Bertana et al., 2021; Hangya et al., 2016; Li & Ma, 2020; Lisi et al., 2021; Locke et al., 2022; Navajas et al., 2017; Sanders et al., 2016). The goal of the current study, therefore, was to investigate a fundamental assumption of Bayesian models of confidence: the use of prior knowledge in the computation of confidence.

46

47

48

49

50

51

52

53

54

55

56

According to Bayesian decision theory, observers combine knowledge about the statistical structure of the world (the “prior”) with the present sensory input (the “likelihood”) to compute a posterior probability distribution over possible states of a stimulus (Drugowitsch et al., 2014b; Hangya et al., 2016; Kepecs and Mainen, 2012; Meyniel et al., 2015; Pouget et al., 2016). The posterior probability distribution, thus, represents every possible observation and its inferred probability. To form a single representation or choice, an ideal Bayesian observer chooses the most likely observation from the posterior probability distribution. According to Bayesian models, confidence can also be derived from this posterior probability distribution and can be defined as the degree of certainty (or probability) associated with the representation that the observer has chosen (or intends to choose; Ma & Jazayeri, 2014).

57

58

59

60

In contrast to Bayesian models, several alternative models of confidence have been proposed. These models posit that confidence reports are better explained by suboptimal computations, suggesting that confidence is based on learned associations with certain *heuristic* cues in the stimulus. These models have received

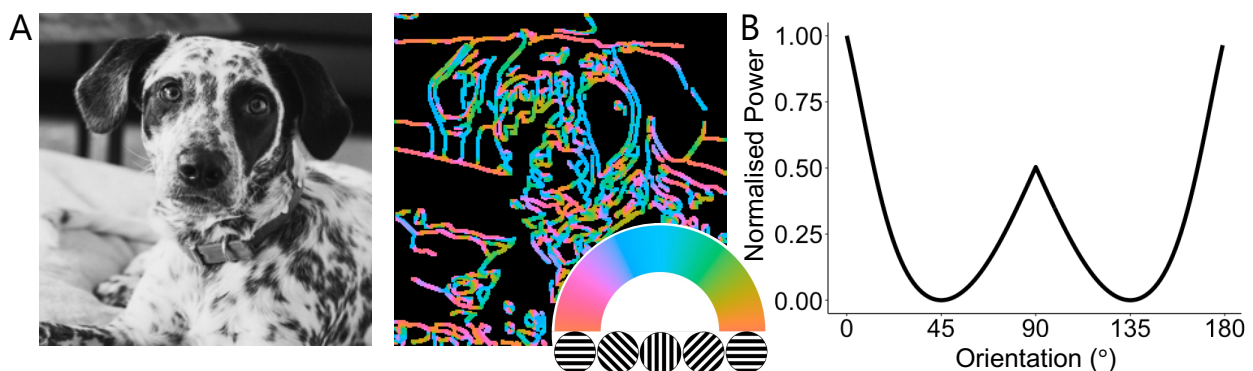
61 some empirical support with a range of studies linking confidence to heuristic cues
62 such as external noise (Bertana et al., 2021; Boldt et al., 2017; Spence et al., 2016),
63 response time (Faivre et al., 2018; Patel et al., 2012; van den Berg, Anandalingam, et
64 al., 2016) and task-difficulty variables (Mole et al., 2018).

65 Despite substantial research interest and myriad explanatory models, the
66 computations underlying the generation of decision confidence remain unclear.
67 Empirical studies investigating the plausibility of Bayesian and non-Bayesian models
68 of confidence have shown mixed results, with some studies finding support for
69 Bayesian models (Aitchison et al., 2015; Li & Ma, 2020; Navajas et al., 2017; Sanders
70 et al., 2016) and others for non-Bayesian models (Adler & Ma, 2018; Aitchison et al.,
71 2015; Bertana et al., 2021; Denison et al., 2018; Lisi et al., 2021; Locke et al., 2022;
72 West et al., 2022). Furthermore, one of the major limitations of existing research is
73 that many previous studies have exposed participants to stimuli drawn from arbitrarily
74 pre-specified prior distributions, and compared their behaviour to that of a Bayesian
75 optimal observer with full knowledge of that distribution (Denison et al., 2018; Li & Ma,
76 2020; Locke et al., 2022; Qamar et al., 2013; West et al., 2022). Such an approach is
77 limited by the ability of humans to internalise the statistics of the prior distribution within
78 the time frame of the experiment (Girshick et al., 2011). If participants are unable to
79 internalise the statistics of the prior distribution within the time-limited context of the
80 experiment, it is unlikely that their confidence judgements will match those of a
81 Bayesian observer, even if priors are otherwise used to inform confidence.

82 To better understand the computations underlying confidence judgements and
83 distinguish among candidate models, in this study we seek to address the extent to
84 which confidence is informed by a prior distribution *without requiring participants to*
85 *learn the parameters of that distribution over the short-term*. Instead, following A-
86 lzzeddin, Mattingley and Harrison (2022), we took advantage of the distributions of
87 low-level features present in naturalistic stimuli to define a prior distribution, the
88 statistics of which have previously been shown to bias humans' perceptual decisions
89 (Appelle, 1972; Berkley et al., 1975; Dakin, 2001; de Gardelle et al., 2010; Girshick et
90 al., 2011).

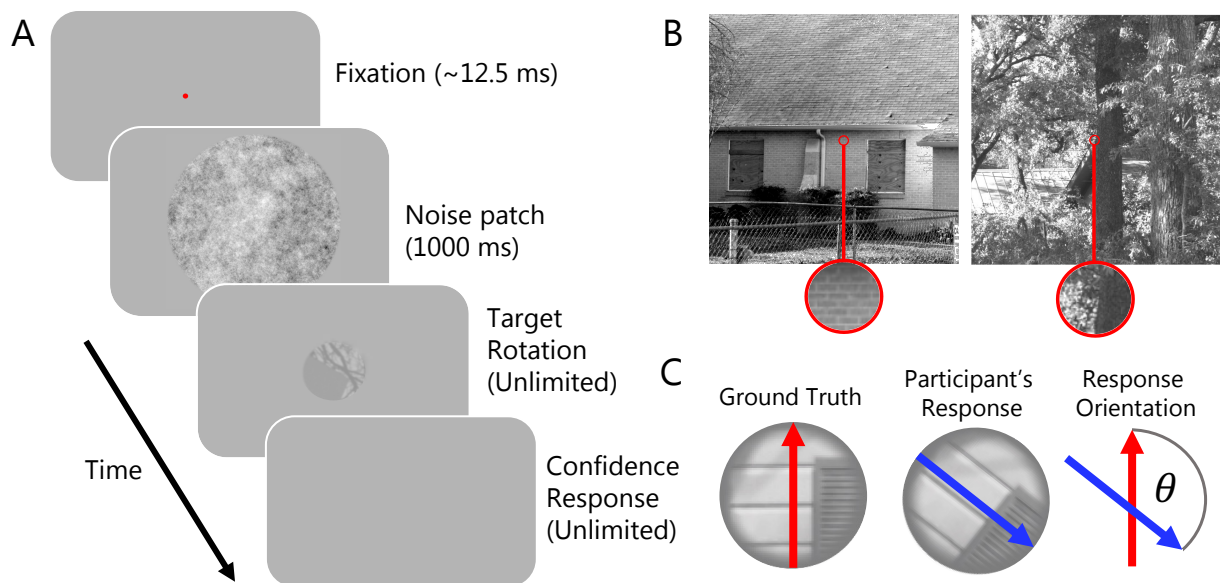
91 A recent study introduced a novel psychophysical paradigm which shows a
92 clear link between environmental statistics and perceptual inferences. A-lzzeddin et

93 al. (2022) presented participants with randomly oriented target images of outdoor
94 scenes and participants were required to infer their subjective “upright” orientation.
95 The targets were designed so that they were windowed within a small aperture of the
96 original image, meaning that the targets themselves contained very little high-level
97 structure. Participants, therefore, had to rely on a strategy which depended on the low-
98 level image features in the targets to judge “upright”. The authors sought to determine
99 if participants had an internal representation of the average distribution of low-level
100 features in the environment, a *prior*, which they used to guide their judgements. For
101 example, as shown in **Figure 1**, horizontal orientation features, and, to a lesser extent,
102 vertical orientation features are over-represented in natural images. A-Izzeddin and
103 colleagues found that participants’ distribution of orientation responses was well
104 approximated by the frequency distributions of orientations in natural images. The
105 authors then used a model observer to show that participants’ responses were
106 explained by a process in which they oriented the targets so that the low-level features
107 in the targets, such as orientation and phase, best approximated the *prior* distribution
108 for these features in the environment. This study, therefore, reveals that *humans have*
109 *an existing, internal model of a prior probability distribution of low-level image statistics*
110 *which they use to inform their perceptual inferences about the world* (A-Izzeddin et al.,
111 2022; see also Girshick et al., 2011). Hence, in the present study, we used the same
112 paradigm to investigate confidence because it allowed us to determine the extent to
113 which participants use an internal prior distribution to compute their confidence without
114 requiring them to explicitly learn the parameters of that distribution.



115
116 **Figure 1. Natural image statistics. (A)** Orientations of edges in digital photos have
117 systematic biases. Original photo taken by Rafael Forseck and used under the
118 Unsplash Licence. **(B)** Idealised distribution of orientations across many natural
119 images (Hansen & Essock, 2004; Harrison et al., 2023).

120 In the present study, participants performed a perceptual task in which they
121 made an orientation judgement about a target image, the *first-order* decision, and then
122 reported their level of confidence in that orientation response, the *second-order*
123 decision (see **Figure 2A**). To investigate whether participants used a prior for natural
124 image statistics when making perceptual and confidence judgements, we used image
125 processing techniques in combination with computational modelling. To preview our
126 results, we confirmed that participants adopted a strategy that aligned the distribution
127 of oriented features and phase with a prior probability model of the distribution of those
128 features in the natural world (A-lzzeddin et al., 2022). Importantly, we also found that
129 participants used a similar prior probability distribution to inform their confidence
130 judgements, even without explicit instruction about the prior. Overall, our findings
131 support a Bayesian characterisation of decision confidence in which its computation
132 depends on multiple features of the incoming sensory information and their
133 consistency with prior probability representations.



134
135 **Figure 2. Experimental paradigm.** (A) Schematic showing trial structure. Participants
136 saw a fixation point, followed by a noise patch and then a target was presented at a
137 random orientation. Participants used the mouse to rotate the target to appear upright
138 and then made a confidence judgement (either “low confidence” or “high confidence”)
139 in their chosen orientation response. (B) Targets, such as the examples outlined in
140 red, were extracted from high quality photos of natural scenes (Burge & Geisler, 2011).
141 (C) To quantify perceptual performance, we computed the angular difference between
142 the objective upright orientation of the target and the participants’ chosen orientation.

143

Results

144

145

146

147

148

149

150

151

To better understand the computations underlying decision confidence, we investigated whether confidence judgements are informed by a prior probability distribution. Rather than requiring participants to learn the statistics of an arbitrary prior distribution, we used a distribution that has been previously shown to affect participants' perceptual inferences: the distribution of orientation energy and phase in natural scenes. To validate this approach, in our first analysis, we confirmed a strong influence of the prior on participants' perceptual judgements as recently reported (A-Izzeddin et al., 2022).

152

Perceptual Judgements

153

154

155

156

157

158

159

160

161

162

163

164

165

166

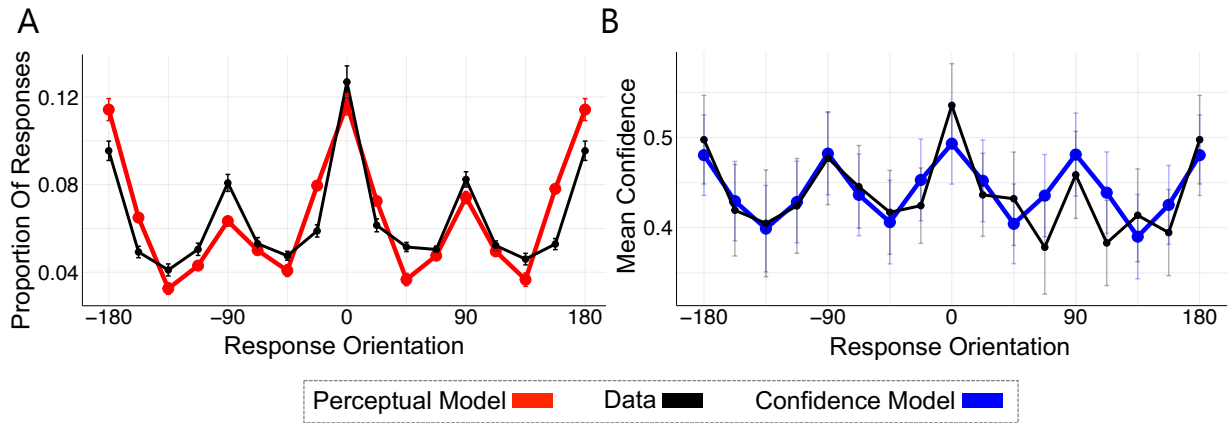
167

168

169

170

To quantify perceptual performance, we computed the angular difference between the objective upright orientation of the target and the participants' chosen orientation, referred to as the *response orientation* (see **Figure 2C**). Response orientation was measured in degrees ranging from -180° to 180° . The black line in **Figure 3A** shows the frequency distribution of response orientations. If participants ($N = 21$) were not able to infer the objective upright orientation of the image using the low-level features in the target, the distribution of response orientations would be distributed uniformly across the range -180° to 180° . By contrast, **Figure 3A** shows that the most frequent response orientation was 0° , suggesting the modal response was highly accurate, and there are clear peaks at the cardinal orientations ($\pm 90^\circ$ and $\pm 180^\circ$), where targets were either inverted relative to their true orientation or offset by 90° . The presence of peaks aligned to cardinal orientations in **Figure 3A** is generally consistent with observers aligning edges within the target to the most common orientations found in nature. Note, however, that observers made $\pm 180^\circ$ inversions less frequently than 0° reports, which requires more than simply aligning the target energy to an orientation prior (in which case there would be an equal proportion of 0° and $\pm 180^\circ$ responses). To further investigate how participants made their responses, we used a model observer, described below.

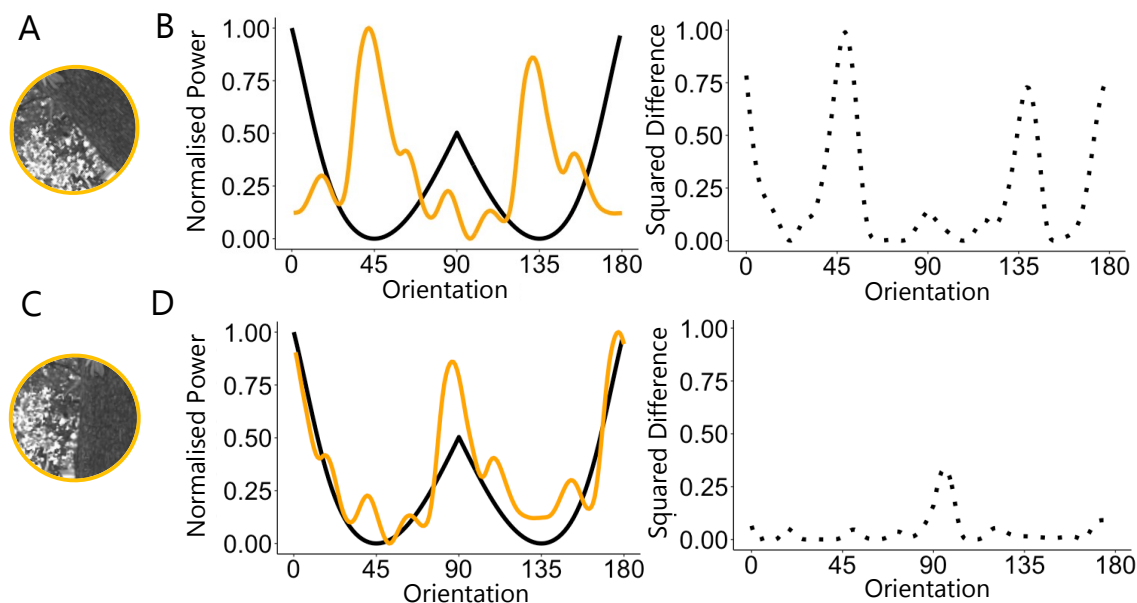


171

172 **Figure 3. Perceptual and Confidence Data and Models (A)** The distribution of
 173 observers' binned response orientations is shown in black. The output of the
 174 perceptual model is shown in red, and provides a good fit to the empirical data. **(B)**
 175 Mean confidence across binned response orientations shown in black. The output of
 176 the confidence model is shown in blue, and provides a good fit to the empirical data.
 177 Bin size = 22.5°. Error bars show ± 1 SEM.

178 ***Perceptual Model***

179 We modelled participants' orientation judgements with a "pretty good observer
 180 model" developed by A-lzzeddin and colleagues (2022; see **Methods** for detailed
 181 model description). Whereas an *ideal* observer model exploits all possible sources of
 182 information to make a decision, the pretty good observer model was designed to use
 183 only a subset of image statistics to make a decision. The model included two stages.
 184 In the first stage, the model rotated the target to best match the distribution of
 185 orientation energy in the target to the prior distribution (see **Figure 4**). In the second
 186 stage, the model used a broadscale filter to estimate the phase of the horizon within
 187 the target, determining if the target needed to be a rotated a further 180°. As described
 188 in more detail by A-lzzeddin et al., the motivation of this second stage was to
 189 approximate a light-from-above prior (Adams, 2007; Brewster, 1826; Metzger, 1936;
 190 Murray, 2013; Ramachandran, 1988). This procedure produced a pattern of modelled
 191 response orientations for the 500 targets shown to each participant. To account for
 192 deviations from the model observer across participants, we fit a single noise parameter
 193 for each participant (see **Methods – Perceptual Model**).



194

195 **Figure 4. Comparison of target distribution of orientation energy and prior**
 196 **distribution. (A)** An example target displayed at an arbitrary orientation. **(B)** Orange
 197 distribution is orientation energy for the target shown in **(A)** compared with the prior
 198 distribution of orientation energy (black). **(C)** The same target as in **(A)**, but rotated to
 199 its objective upright. **(D)** Orange distribution is orientation energy for target shown in
 200 **(C)**, compared with the prior distribution of orientation energy (black). Right panels of
 201 **(B)** and **(D)** show squared difference in normalised power between the target and the
 202 prior for each orientation bin. The perceptual model rotates the target to minimise the
 203 sum of the squared differences across all orientation bins.

204 As shown in **Figure 3A**, the perceptual model provided a very good
 205 approximation of participants' responses. The close correspondence between
 206 participants' responses and model responses suggests that participants judge the
 207 orientation of the target by matching a relatively simple set of low-level image statistics,
 208 namely orientation energy and phase, to an internal representation of the distribution
 209 of these statistics in the natural world. Thus, we confirmed that participants use prior
 210 knowledge of natural image statistics to make novel perceptual inferences about
 211 ambiguous stimuli (A-Izzeddin et al., 2022).

212 Confidence Judgements

213 If participants' confidence was informed by the same prior used to make their
 214 perceptual orientation inferences, we hypothesised that their confidence judgements
 215 should characterise how well they had matched the low-level statistics in the target
 216 with the prior. In contrast, if participants did not use the prior to inform their confidence,
 217 their confidence judgements would depend on other heuristic cues, not related to the

218 prior. We tested these predictions with a second model, the confidence model,
219 described below. We first provide an overview of the average distribution of confidence
220 responses across response orientations and then outline the assumptions and
221 performance of the confidence model.

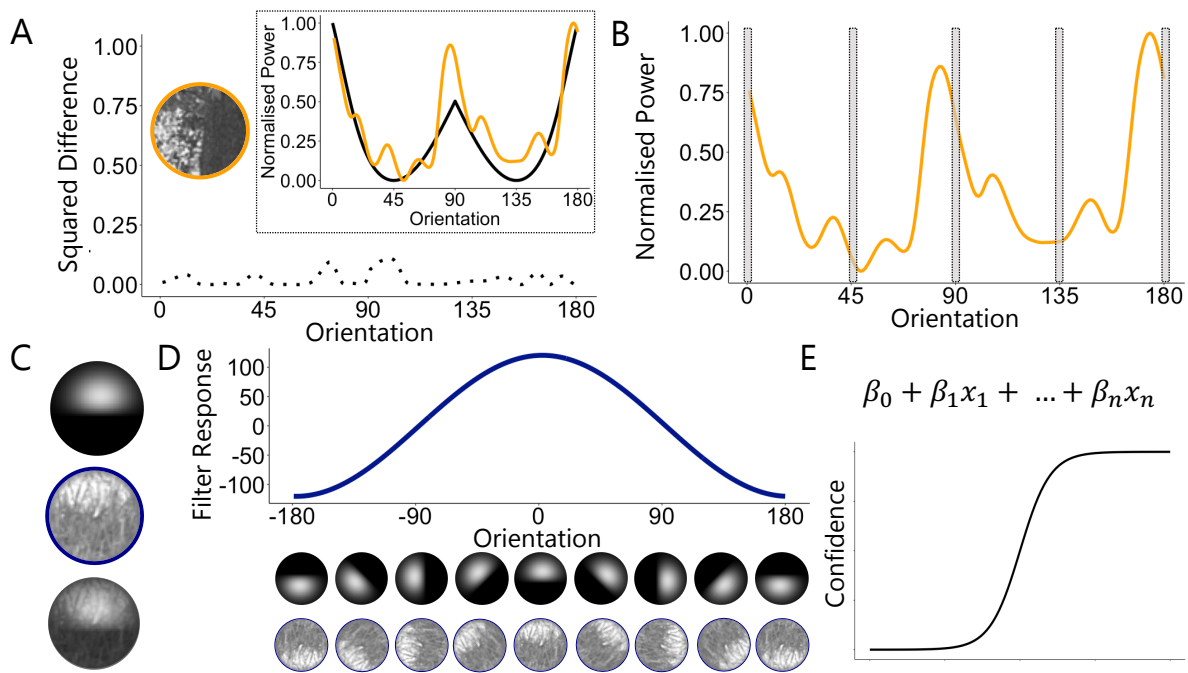
222 The black data in **Figure 3B** shows mean confidence as a function of response
223 orientations. Participants were most confident in their most accurate orientation
224 responses (responses in the 0° bin), suggesting they had some metacognitive
225 awareness of the match of their perceptual judgements to the upright image. There
226 are also clear peaks in confidence at the cardinals ($\pm 90^\circ$ and $\pm 180^\circ$), demonstrating
227 that participants' confidence responses show the same cardinal biases as the
228 perceptual judgements. Our perceptual model revealed that participants use priors for
229 the distribution of orientation energy and phase in natural scenes to inform their
230 orientation judgements. We therefore wanted to develop a similar statistical model to
231 determine if participants' confidence judgements were informed by the same prior.

232 ***Confidence Model***

233 For the confidence model, we developed several measures that summarised
234 the degree of overlap in orientation energy and phase in the target and the prior. In
235 addition to these prior-related measures, we also considered the possibility that
236 confidence depends on other stimulus cues not related to the prior, such as the
237 contrast of the target patch or response time of the first-order decision (Bertana et al.,
238 2021; Boldt et al., 2017; Faivre et al., 2018; Mole et al., 2018; Patel et al., 2012;
239 Spence et al., 2016; van den Berg, Anandalingam, et al., 2016). To relate these
240 measures to confidence and investigate their relative importance, we used a
241 generalised linear mixed model framework in the form of a modified logistic regression.
242 This allowed us to use a set of weighted stimulus variables to predict binary confidence
243 responses. We describe the assumptions of each predictor in the model and the fixed
244 effect of that predictor below. See **Methods – Confidence Model** for further model
245 description. See **Supplementary Table 1 and Supplementary Figure 2** for model
246 parameters and predictions. See **Supplementary Figure 5** for the correlation between
247 fixed effects.

248 **Orientation Energy.** We tested two different assumptions about how
249 participants may quantify the degree of overlap between the distribution of orientation

250 energy in the target and the prior. These assumptions were quantified in what we refer
251 to as the *prior mismatch predictor* and the cardinal and oblique orientation *energy*
252 *predictors*. For the prior mismatch predictor, we assumed that participants directly
253 compared a continuous representation of the distribution of orientation features in the
254 stimulus and veridical knowledge of the prior distribution of orientation energy (see
255 **Figure 5A**). The prior mismatch predictor, therefore, was a single statistic that
256 summarised the difference between the entire distribution of orientation energy in the
257 target at the rotational offset chosen by the observer and the prior. As shown in **Figure**
258 **6B**, however, the effect of the prior mismatch predictor on confidence was not
259 significant ($e^{\beta} = 0.95$, 95% *CI* [0.88, 1.04], $p = 0.261$), suggesting that participants do
260 not appear to explicitly compare the distribution of orientation energy in the target and
261 the prior veridically.



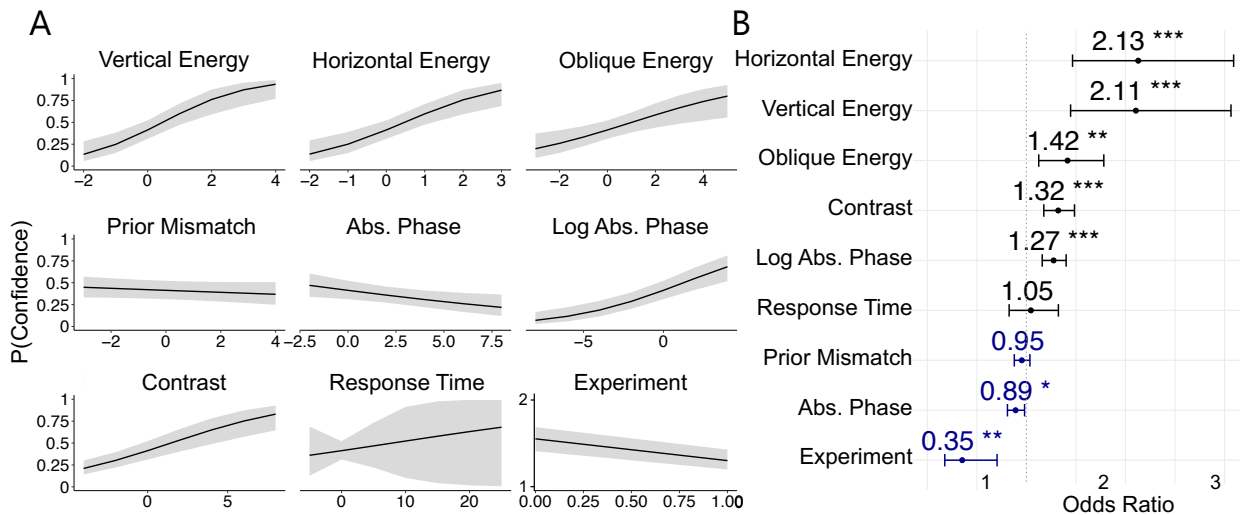
263

264 **Figure 5. Prior Predictors for Confidence Model.** (A) Example difference in
 265 orientation energy for each bin between the distribution for the target (orange
 266 distribution in inset) and the prior (black distribution in inset). The sum of these
 267 differences was used as the *prior mismatch predictor* in the confidence model. (B)
 268 Example distribution of orientation energy with horizontal (0° or 180°), vertical (90°)
 269 and oblique (45° or 135°) energy shaded. These values were calculated for each target
 270 at the rotational offset chosen by the observer and used to predict confidence. (C)
 271 Example of a broadscale filter with a positive polarity (top circle) and an example target
 272 (middle circle). The filter is applied to the target (bottom circle) to determine the
 273 direction and strength of lighting in the target. (D) Example response of a broadscale
 274 filter (blue distribution in plot). The broadscale filter is positioned at different rotational
 275 offsets (top row) based on the orientation of the target (bottom row). The response of
 276 the filter at the offset chosen by the observer was used as a predictor in the confidence
 277 model. (E) Linear predictors were passed through an inverse logistic link function to
 278 predict confidence responses.

279 As an alternative to computing confidence by comparing the full prior probability
 280 distribution of orientation energy with that measured from the target, we postulated
 281 that observers might instead be most confident in targets that contain strong vertical
 282 or horizontal features, based on their internal model of the over-representation of these
 283 features in natural scenes. We therefore included a second set of predictors in the
 284 confidence model which quantified the amount of vertical (where $\theta = 90^\circ$), horizontal
 285 energy (where $\theta = 0^\circ$ or 180°) and oblique energy (where $\theta = 45^\circ$ or 135°) in the
 286 target at the rotational offset chosen by the participant (see **Figure 5B**). We found that
 287 vertical orientation energy ($e^\beta = 2.13$, 95% CI [1.47, 3.09], $p < .001$), horizontal

288 orientation energy ($e^\beta = 2.11$, 95% *CI* [1.45, 3.06], $p < .001$) and oblique orientation
289 energy ($e^\beta = 1.42$, 95% *CI* [1.12, 1.78], $p = .003$) were all positively predictive of
290 confidence. The effect of vertical and horizontal energy was almost twice that of
291 oblique orientation energy (see **Figure 6B**), suggesting that participants most heavily
292 weight the over-representation of vertical and horizontal features in natural scenes to
293 inform their confidence.

294 **Phase.** Orientation energy is phase invariant, and so a participant cannot use
295 orientation energy alone to distinguish a 0° and $\pm 180^\circ$ target. We therefore used a set
296 of predictors in the confidence model that estimated phase (see **Methods**). We used
297 the response of a broadscale filter positioned in the centre of the target at the rotational
298 offset chosen by the observer as a phase, which we take to be indicative of the
299 strength of a directional lighting signal. We used both the absolute value and a log
300 transformed value of absolute phase in the confidence model to allow for non-linear
301 relationships between target phase and confidence. The effects of absolute phase
302 ($e^\beta = 0.89$, 95% *CI* [0.81, 0.98], $p = .020$) and log transformed absolute phase on
303 confidence were significant ($e^\beta = 1.32$, 95% *CI* [1.18, 1.49], $p < .001$). The effect of
304 the log transformed absolute phase on confidence suggests that the relationship
305 between target phase and confidence was non-linear. This relationship is also positive
306 such that the more evidence that there was a strong source of lighting in the target,
307 the more confident the participant was in their response. Overall, these findings
308 suggest that participants use low-level features such as the phase of the target, which
309 can approximate the strength of a light source in the image, to inform their confidence.



310

311

312

313

314

315

316

317

Figure 6. Confidence Model. (A) Marginal fixed effects of each predictor on confidence. Shaded regions show ± 1 standard error of the predictions. Note that predictors vertical energy, horizontal energy, oblique energy, prior mismatch, absolute phase, log absolute phase, contrast and response time were standardised. **(B)** Odds ratio for fixed effects. Dotted vertical line indicates odds ratio of 1. Error bars show 95% confidence intervals. Blue values indicate negative coefficients. *** $p < .001$, ** $p < .01$, * $p < .05$.

318

Other predictors. If, contrary to the above effects of orientation energy and

319

phase, participants did not use the prior to inform their confidence, we hypothesised

320

that they might use other heuristic-like cues. We therefore included two predictors in

321

the confidence model that were not directly related to the prior: the overall contrast of

322

the target patch (RMS contrast) and the response time of the first-order decision.

323

The effect of response time on confidence was not significant ($e^\beta = 1.05$,

324

95% CI [0.83, 1.32], $p = .721$), suggesting that participants do not use their first-order

325

response time as a heuristic cue for confidence. The effect of contrast on confidence,

326

however, was significant ($e^\beta = 1.27$, 95% CI [1.16, 1.40], $p < .001$), where increasing

327

target contrast was predictive of increasing confidence. Considering the strong effect

328

of oriented contrast energy on confidence reports, it is not particularly surprising that

329

a measure of isotropic orientation was also a significant predictor. Indeed, RMS

330

contrast was moderately correlated with vertical and horizontal energy (see

331

Supplementary Figure 5). However, this finding could nonetheless also suggest that,

332

over and above the effect of priors, participants use other stimulus features to compute

333

their confidence.

334 To visualise how well these measures accounted for the data more generally,
335 we generated predictions for a model using the statistically significant predictors only
336 ($p < 0.05$ in **Figure 6**; horizontal orientation energy, vertical orientation energy, oblique
337 orientation energy, absolute phase, log absolute phase, contrast and experiment; see
338 **Supplementary Table 2**). The predicted confidence from this model is shown in
339 **Figure 3B** (blue distribution). The model describes the empirical confidence data very
340 well (black distribution; **Figure 3B**), capturing the major peaks in confidence at the
341 cardinal orientations. To provide a reference point for model performance, we fit an
342 intercept only model with an intercept term for each participant (see **Supplementary**
343 **Figure 3** and **Supplementary Table 3**). We found substantially poorer performance
344 for the intercept model ($AIC_{intercept} = 12657.19$, $BIC_{intercept} = 12678.97$, $AIC_{conf} =$
345 12099.96 , $BIC_{conf} = 12361.29$; see **Supplementary Figure 4**). This finding suggests
346 that the confidence model, with the predictors that quantify the low-level features in
347 the targets and their degree of overlap with the prior, was more useful for explaining
348 variations in confidence than a constant value for confidence for each participant.

349 Despite capturing many aspects of participants' confidence reports, the model
350 is incomplete. As shown in **Figure 3B**, the confidence model underpredicts confidence
351 for correctly oriented targets (those with response orientations of 0°), suggesting that
352 observers may have had access to other features in the targets, not captured by the
353 model, which led them to confidently infer the correct upright orientation of the target.
354 The model also appears to overpredict confidence for response orientations between
355 ~ 65 - 165° . We expect that this asymmetry in the confidence data, where the pattern of
356 responding is different for response orientations of ~ 65 - 165° and ~ 165 - 65° , is a result
357 of non-stimulus-specific noise that is not captured by the model. Despite these minor
358 limitations, a small set of environmental statistics provides a reasonable basis from
359 which to understand confidence computations.

360 **Discussion**

361 We investigated the influence of priors on decision confidence. Observers
362 performed a task in which they rotated a naturalistic image patch to its upright
363 orientation, the *first order decision*, and then made confidence judgements in their
364 orientation responses, the *second order decision*. We found that participants use
365 internal priors about the statistical regularities of low-level features in natural scenes

366 to make their perceptual judgements, replicating a recent investigation (A-Izzeddin et
367 al., 2022). Importantly, we also found that participants use the same priors to inform
368 their confidence responses, even without explicit instruction about the prior. We
369 discuss the implication of these findings for our understanding of decision confidence
370 below.

371 **Priors Affect Confidence**

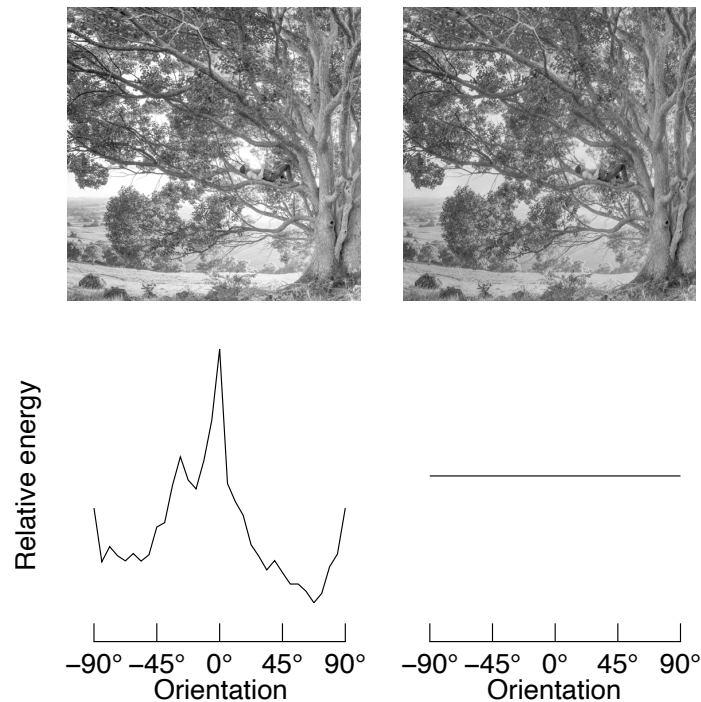
372 We found that participants use prior knowledge about the statistical regularities
373 of orientation energy and phase in natural scenes to inform both their perceptual
374 inferences and confidence judgements. In the following sections, we discuss the role
375 of this information in models of confidence.

376 ***Orientation Energy***

377 Our confidence modelling results showed that the amount of vertical and horizontal
378 orientation energy in the target was an important predictor of confidence. In fact, the
379 effect of vertical and horizontal energy on confidence was almost twice that of oblique
380 orientation energy. Participants were not given any instruction about which image
381 features to use to make their judgements and were not given any explicit instruction
382 about a prior distribution. This finding, therefore, suggests that participants appear to
383 use implicit knowledge about the over-representation of horizontal and vertical
384 orientation features in natural scenes to inform their confidence. This finding broadens
385 our understanding of the influence of the statistical regularities of orientation features
386 in natural scenes on perceptual judgements (Appelle, 1972; Berkley et al., 1975;
387 Campbell et al., 1966; Dakin & Watt, 1997; Girshick et al., 2011; Hansen et al., 2003,
388 2008; Pratte et al., 2016) and demonstrates, for the first time, that these low-level
389 perceptual priors also effect observers' confidence.

390 Although participants appear to use knowledge about the prior probability of certain
391 oriented features in natural scenes to inform their confidence, we did not find evidence
392 that participants directly compare a full prior probability distribution of orientation
393 energy in natural scenes and the distribution of orientation energy in the target directly
394 (the *prior mismatch* predictor). Instead, our results suggest that participants use only
395 a subset of orientations to inform their confidence, or, alternatively, use orientations
396 within only some spatial frequencies. This finding suggests that perhaps observers
397 may not use the entire prior probability distribution but instead, confidence is informed

398 by only the most predictive features of the prior. As shown in **Figure 7**, perceptually
399 apparent cardinal structures need not be defined by peaks in energy as defined in our
400 prior. When quantifying energy, we aggregated over all spatial frequencies, whereas
401 human vision is known to be bandpass (Campbell & Robson, 1968). Future models
402 could therefore weight an image's orientation energy according to the human contrast
403 sensitivity. Furthermore, phase alignment at different spatial scales is critical to
404 perceptually relevant edge features that can guide the sorts of perceptual and
405 confidence decisions in our study (Rideaux et al., 2022a). We discuss the role of phase
406 in confidence computations in the next section.



408

409 **Figure 7. Informativeness of Full Prior Distribution.** Comparing the full distribution
 410 of orientation energy to a prior may not always be functional. The image on the left
 411 shows a greyscale natural image. Its orientation energy is shown below the image,
 412 and closely matches the prior distribution shown in **Figure 1**. The image on the right
 413 is the same image, but we have “whitened” its amplitude spectrum with respect to
 414 orientation: as shown below the image, the modified image has equal energy at all
 415 orientations. Despite the large change in orientation energy, the images are
 416 perceptually similar. Because natural images are dominated by low-spatial frequency
 417 structures, energy within low spatial frequency bands were over-represented in our
 418 measure of orientation energy relative to the bandpass properties of human vision.
 419 However, this example nonetheless demonstrates that clearly oriented cardinal
 420 structures need not be defined by peaks in energy as defined in our prior per se.
 421 Instead, phase alignment at different spatial scales, and orientation energy within
 422 different spatial frequency sub-bands, are critical to perceptually relevant edge
 423 features that can guide the sorts of perceptual and confidence decisions in our study
 424 (Rideaux et al., 2022b).

425

426 **Phase**

427 Because orientation energy is phase-invariant, we included a set of predictors in
 428 the confidence model that estimated the phase of the horizon in the target in order to
 429 capture a proportion of responses that were inverted by 180°. We found a non-linear
 430 effect of the phase predictor on confidence such that the more evidence that there was
 431 a clear horizon in the target, the more confident participants were in their response.

432 The horizon in the target could be used to approximate both the direction and strength
433 of lighting in the target. Lighting in the natural world is known to follow certain statistical
434 regularities, mostly originating from above the horizon due to predominant sources of
435 illumination being the sun and overhead lights. The demonstrated effect of phase on
436 confidence is thus consistent with well documented perceptual effects that humans
437 have priors for the direction of lighting in natural scenes (Adams, 2007; Brewster,
438 1826; Metzger, 1936; Murray, 2013; Ramachandran, 1988) and provides converging
439 evidence that participants use priors based on experience with the statistical
440 regularities of the natural world to inform their confidence.

441 **The Computational Basis of Confidence**

442 Our finding that priors are demonstratively used to inform confidence helps to
443 resolve some of the theoretical debate about the computational basis of confidence.
444 One of the leading theories of confidence suggests that it is computed according to
445 the rules of Bayesian inference where humans combine a *prior* with a *likelihood* to
446 compute a *posterior probability distribution*. Currently, however, the evidence for
447 Bayesian accounts of confidence have been mixed with some studies finding evidence
448 for Bayesian models (Aitchison et al., 2015; Li & Ma, 2020; Navajas et al., 2017;
449 Sanders et al., 2016) and others for non-Bayesian models (Adler & Ma, 2018;
450 Aitchison et al., 2015; Bertana et al., 2021; Denison et al., 2018; Lisi et al., 2021; Locke
451 et al., 2022). One of the major limitations of existing research, however, is that many
452 previous studies have assumed participants' effective internalisation of arbitrary prior
453 distributions and compared their behaviour to that of a Bayesian optimal observer with
454 full knowledge of that distribution (Denison et al., 2018; Li & Ma, 2020; Locke et al.,
455 2022; Qamar et al., 2013; West et al., 2022). This assumption is rarely interrogated,
456 despite the fact that if observers are unable to internalise the statistics of the prior
457 distribution within the time-limited context of the experiment, it is unlikely their
458 confidence judgements will match that of a Bayesian observer. This would make it
459 difficult to find evidence of the use of priors in confidence judgments even if priors are
460 used to inform confidence beyond the lab.

461 In this study, we used a task design in which we did not need to explicate a prior
462 distribution and could instead rely on participants' existing priors. Such a task allowed
463 us to confirm that priors do indeed influence confidence responses. Our findings are

464 consistent with a Bayesian characterisation of confidence in which confidence
465 depends on prior information, although further development of our models is required
466 in order to compute a full posterior distribution as per other Bayesian formulations
467 (Aitchison et al., 2015; Li & Ma, 2020; Navajas et al., 2017; Sanders et al., 2016;
468 Denison et al., 2018; Locke et al., 2022; West et al., 2022). Our demonstration of the
469 importance of priors suggests that previous research showing evidence *against*
470 Bayesian models of confidence should be interpreted with caution. It is feasible that
471 the use of arbitrary prior distributions in previous research meant that participants were
472 unable to internalise the statistics of those distributions veridically and thus showed
473 systematic deviations from prior-informed optimal behaviour. Our findings imply that
474 future studies evaluating the computational basis of confidence could rely more on
475 naturalistic task designs or use computational models that allow for inaccurate
476 knowledge about the prior distribution.

477 **Other Stimulus Features as Cues for Confidence**

478 In addition to the effect of priors on confidence, we investigated if participants
479 used other cues to inform their confidence. Inconsistent with some previous research,
480 we did not find evidence that response time in the first order decision influenced
481 confidence (Faivre et al., 2018; Patel et al., 2012; van den Berg, Anandalingam, et al.,
482 2016). We did, however, find that the contrast of the target had a significant effect on
483 confidence, where higher target contrast was associated with greater confidence. We
484 postulate that stimulus contrast in our experimental paradigm may provide an
485 important cue about sensory uncertainty. Lower contrast targets provide less clear and
486 consistent visual information (Bex & Makous, 2002), and, therefore, contrast can
487 provide a meaningful cue about the perceptual uncertainty of the source of information
488 on which the decision is based. This is consistent with studies showing that confidence
489 is influenced by perceived sensory uncertainty (Adler & Ma, 2018; Denison et al.,
490 2018; Michael et al., 2015; West et al., 2022). Furthermore, it is generally consistent
491 with theoretical work which links confidence with the hypothesis that perceptual
492 uncertainty is encoded as the variance in firing rates across neural populations, with
493 increased uncertainty leading to down-weighting of that evidence source in perceptual
494 integration (Beck et al., 2008; Ma et al., 2006). Further research is required to confirm

495 these hypotheses and understand the neural mechanisms by which certain stimulus
496 features, like image contrast, are involved in the computation of confidence.

497 **Conclusions**

498 Our results support the idea that observers combine multiple features of
499 incoming sensory information with prior probability representations to compute their
500 confidence. Our experimental paradigm capitalises on statistical regularities in the
501 structure of natural scenes such that participants relied on an existing, internal
502 representation of prior probabilities to make their judgements. This meant that, unlike
503 previous research, incomplete knowledge about the statistics of the prior distribution
504 would not bias our interpretations about the computational basis of confidence. Our
505 results provide important evidence supporting a Bayesian characterisation of
506 confidence, highlighting the joint influence of priors and other perceptual features,
507 such as sensory uncertainty, on confidence. Overall, our study demonstrates that prior
508 knowledge plays an important role in both the perceptual and metacognitive decisions
509 that humans make about the noisy, ambiguous sensory information they encounter
510 every day.

511 **Methods**

512 **Overview.** On each trial, a participant viewed a randomly oriented *target*,
513 positioned in the centre of the display (see **Figure 2A**). The participant was informed
514 that the target was a circular patch that had been cropped from the centre of a larger
515 *source image*, where source images were randomly selected from a database of
516 images of outdoor scenes (see **Figure 2B**). The participant was instructed to rotate
517 the target to the “upright” orientation, with no additional contextual information given
518 about the source image. For each target, the participant made their orientation
519 judgement, the *first order decision*, and then made a confidence judgement in their
520 chosen orientation response, the *second order decision*, reporting either “high
521 confidence” or “low confidence”.

522 **Participants**

523 In total, 21 participants ($M_{age} = 23.95$, $SD_{age} = 4.65$; no exclusions) completed
524 the experiment. 10 participants completed Study 1 and 11 participants completed
525 Study 2. All methods were the same for Study 1 and Study 2, unless indicated

526 otherwise. As there did not appear to be any clear differences in the results of Study
527 1 and Study 2, we combined datasets across studies. We, therefore, report results for
528 all 21 participants. See **Supplementary Material: Experiment 1 and Experiment 2**
529 **Comparison** for additional commentary. All participants were naïve to the purpose of
530 the study and were reimbursed for their time (\$20 per hour in cash). Ethics approval
531 was granted by the University of Queensland Medicine, Low & Negligible Risk Ethics
532 Sub-Committee.

533 **Stimuli & Apparatus**

534 All participants saw the same 500 digital natural images, selected randomly
535 from a database of high-resolution photos of outdoor scenes and cropped to
536 1080x1080 pixel regions (Geisler & Perry, 2011; A-lzzeddin et al., 2022). Targets
537 were circular patches cropped from the centre of the 1080x1080 images, subtending
538 2° of visual angle in diameter (see **Figure 2B**). All stimuli were converted to greyscale
539 using MATLAB's `rgb2gray()` function. During practice, targets were selected randomly
540 from a different set of images from the same database.

541 Stimuli were presented using the Psychophysics Toolbox (3.0.12; Brainard,
542 1997; Pelli, 1997) and a gamma correction was applied to the display, assuming
543 gamma was 2. In Study 1, stimuli were presented on a 24-inch ASUS VG428QE
544 monitor, 1920 x 1080-pixel resolution and a refresh rate of 100 Hz. Participants were
545 seated in a dark room with their head positioned on a chin rest fixed at a viewing
546 distance of 57cm. In Study 2, stimuli were presented on a 24-inch DELL P2414H
547 monitor, 1920 x 1080-pixel resolution and a refresh rate of 60 Hz.

548 **Procedure**

549 As shown in **Figure 2A**, at the start of each trial participants were presented
550 with a central fixation point for ~125 ms (fixation time sampled from a uniform
551 distribution between 0 and 250 ms) followed by a black and white pink noise patch for
552 1000 ms (27° of visual angle in diameter). The target was then presented centrally at
553 a random orientation and participants used the mouse to re-orient the patch to be
554 “upright”. Participants clicked the mouse to confirm their response and then used the
555 arrow keys (left arrow = low confidence and right arrow = high confidence) to indicate
556 their confidence in their chosen orientation. Half of the participants were instructed to
557 use the high confidence and low confidence ratings approximately equally often (Study

558 1) and the other half of participants received no additional instructions about using the
559 confidence ratings (Study 2). All participants completed 500 trials with the same
560 targets, the order of which was randomised for each participant. Trials were split into
561 5 blocks of 100 trials with self-paced breaks in between blocks.

562 Prior to completing the experiment, participants did 40 practice trials to
563 familiarise themselves with the task. In the first 20 practice trials, participants only
564 rotated the targets to their “upright” orientation and, in the remaining 20 trials,
565 participants rotated the targets and then made confidence ratings. Participants saw
566 different target images during testing and training.

567 **Data Analyses**

568 We used statistical models and digital signal processing techniques (e.g.
569 Harrison, 2022) to investigate whether participants use a prior for natural image
570 statistics when making perceptual inferences. We then developed a novel statistical
571 model to determine if participants use the same prior to inform their confidence
572 judgments. In the following sections, we first describe the image processing methods
573 used to derive the distribution of orientation energy and phase for the prior and each
574 target patch. We then describe the perceptual and confidence models.

575 The targets were designed so that they were windowed within a small aperture
576 of the larger source image. This meant that the targets themselves contained very little
577 high-level structure that participants could use to unambiguously infer the upright
578 orientation of the target (see **Supplementary Material: High-Level Image Features**
579 **and “Informativeness” Data** for further discussion on this issue). Participants,
580 therefore, had to rely on a strategy that depended on the low-level image features in
581 the targets only (see **Supplementary Figure 8**). Based on A-Izzeddin and colleagues
582 (2022), we expected that participants would adopt a strategy in which they chose
583 rotational offsets for the targets which best matched the distribution of low-level
584 features in the targets to the average distribution of these features in the environment,
585 referred to as the *prior*. Consistent with A-Izzeddin and colleagues (2022), we focused
586 on the use of two specific low-level features, the distribution of orientation energy and
587 phase, and defined the prior as the average distribution of these features across
588 thousands of images of natural scenes (see **Figure 1**). Importantly, for the
589 experimental task, we did not provide any guidance on what features participants

590 should use to make their decisions or give them any explicit instructions about the
591 prior. Instead, we relied on participants' *internal* representation of the prior to do the
592 task.

593 **Orientation Energy**

594 **Prior.** We defined the prior distribution of orientation energy based on studies
595 of natural images (e.g. Wei & Stocker, 2015):

$$p(\theta) \propto 2 - |\sin\theta| \quad (1)$$

596 where $p(\theta)$ is the probability of observing orientation energy with an orientation of θ in
597 radians. Equation **Error! Reference source not found.** assumes equal prevalence of
598 horizontal and vertical orientations. Other studies, however, have shown that
599 horizontal features are over-represented relative to vertical features (Hansen et al.,
600 2003; Hansen & Essock, 2004; Harrison, 2022). We therefore modified Equation
601 **Error! Reference source not found.** by increasing the proportion of horizontal energy
602 according to a von Mises function which was normalised to have a peak of one:

$$p(\theta) \propto 2 - |\sin\theta| + C \exp(\kappa(\cos\theta - 1)) \quad (2)$$

603 where C is the strength of the horizontal bias, and κ is the width of the von Mises
604 function which we set to 2.5. $p(\theta)$ was then normalised within the range 0 – 1. Small
605 changes in κ did not change the results. **Figure 1** shows the prior distribution of
606 orientation energy (black distribution).

607 **Target Patch.** We calculated the distribution of orientation energy in the target
608 to compare against the prior. For a given target patch, we computed orientation energy
609 in 180 equally space orientation bands, each of which covered all spatial frequencies.
610 These operations were performed in the frequency domain; energy was the absolute
611 of the Fourier-transformed target patches. Orientation filters were also constructed in
612 the frequency domain as raised cosine filters with a bandwidth of 45° (full width half
613 height). Energy was summed within each orientation band, giving a distribution of
614 energy across orientations. Because absolute energy fluctuates from one image to the
615 next, the distribution of energy was normalised within the range 0 – 1, by subtracting
616 the minimum value, and then dividing by the maximum value. **Figure 4B/D** shows

617 example distributions of orientation energy (orange distribution) for an example target
618 patch at two different rotational offsets in **Figure 4A/C**.

619 **Phase**

620 As described in A-Izzeddin et al. (2022), contrast energy alone is circular
621 around $\pm 90^\circ$, whereas observers' reports are circular around $\pm 180^\circ$. To estimate fully
622 circular responses, therefore, a second image statistic is required to determine
623 whether an image needs to be inverted. We modelled this process as an estimate of
624 the phase of the horizon.

625 **Prior.** Consistent with previous research, we assumed that participants had a
626 light-from-above prior (Adams, 2007; Brewster, 1826; Metzger, 1936; Murray, 2013;
627 Ramachandran, 1988). In other words, we assumed that the response of a broadscale
628 filter positioned in the centre of the target should on average, be positive, consistent
629 with light being above the horizon in naturalistic scenes.

630 **Target Patch.** To measure the phase of the target on a given trial, the
631 broadscale filter was positioned in the centre of the target and at the orientation of the
632 rotational offset of the target. The polarity of the response of the filter was used to
633 determine lighting direction. That is, if the response of the filter was positive, light would
634 appear to be above the horizon in the target and if the response of the filter was
635 negative, light would appear to be below the horizon in the target (see **Figure 5C**).

636 **Perceptual Model**

637 We used the model observer developed by A-Izzeddin and colleagues (2022)
638 to investigate whether participants use an internal prior model for low-level image
639 features to inform their orientation judgements. This model is defined as a "pretty good
640 observer" model because it uses a subset of image statistics to make a decision, as
641 opposed to an "ideal observer" model which exploits all possible sources of
642 information.

643 The model included two stages. In the first stage, we rotated the target to best
644 match the distribution of orientation energy in the target with the prior. We used
645 MATLAB's `fminsearch()` function to find the rotational offset that minimised the sum of
646 squared differences in each orientation band between the target and the prior (see
647 **Figure 4**). To avoid local minima, we fit the model with varying starting parameters
648 and used the rotational offset at the global minimum from all fits. Because orientation

649 contrast is phase invariant, in the second stage of the model after finding the best
650 rotational offset, we estimated lighting direction in the patch using a broadscale filter
651 and inverted the target so that it was consistent with a light-from-above prior, as
652 described above. In other words, where the response of the filter was positive, the
653 model observer would leave the target patch at the current orientation. If, on the other
654 hand, the phase was negative, the model observer would rotate the target patch by
655 180°. The stronger the absolute value of the phase response, the more evidence the
656 model observer had about the horizon.

657 The fitting of the perceptual model as described thus far was independent from
658 participants' responses – we fit the targets' statistics to the prior. This meant that the
659 model was deterministic. Because all participants saw the same targets, the model
660 predicted the same pattern of responses for all participants. To account for deviations
661 from the model observer across participants, we fit a single noise parameter for each
662 participant: we added a random amount of noise, ε , to the model's predicted response
663 orientation for each target. The amount of added noise was sampled from a normal
664 distribution with a mean of 0 and a standard deviation, σ , that was estimated
665 separately for each participant, j , such that:

$$N(\varepsilon; 0, \sigma_j) \tag{3}$$

666 where N denotes the normal density function and ε is the amount of noise added to
667 the perceptual model's prediction. We estimated σ by minimising the difference
668 between each participant's observed distribution of response orientations and the
669 mean predicted distribution of response orientations for that participant using ordinary
670 least squares according to:

$$\sum_b (\delta_{j,b} - \rho_{j,b})^2 \tag{4}$$

671 Where δ is the observed proportion of responses and ρ is the predicted proportion of
672 responses in bin, b , for participant, j . To calculate the predicted proportion of
673 responses, we simulated 1000 noisy responses by drawing random samples of ε
674 according to Equation 3 for each trial and each participant and added these random
675 samples to the model's predicted orientation response for that target. We then

676 calculated the average proportion of responses in each orientation bin for each
677 participant. See **Supplementary Table 4** for σ parameter estimates.

678 **Confidence Model**

679 For the associated confidence judgements, we sought to determine if
680 participants use the same prior for the distribution of low-level features in natural
681 scenes to inform their confidence. If participants use the same perceptual prior to
682 inform their confidence, we hypothesised that their confidence judgements would
683 reflect how closely the distribution of low-level features in their chosen orientation
684 response matched the prior distribution. To test this prediction, we developed several
685 measures that summarised the degree of overlap in orientation energy and phase in
686 the target, as oriented by the participant, and the prior (described above). In contrast
687 to these prior-related measures, we also considered the possibility that confidence
688 depends on other stimulus cues not related to the prior, such as the contrast of the
689 target patch or response time of the first-order decision. To evaluate these predictions,
690 we used a generalised linear mixed model framework to investigate the relationship
691 between certain features of the target and participants' confidence judgements.
692 Importantly, we computed the measures (described in detail below) using the targets
693 at the rotational offset chosen by the participant on each trial, reflecting the fact that
694 confidence judgements are a second-order reflection on the first-order decision.

695 In the sections below, we first describe the general modelling framework (the
696 generative model) and then describe each of the measures used to predict confidence.

697 **Generative Model**

698 We used a generalised linear mixed model (GLMM) in the form of a modified
699 logistic regression to relate a set of weighted predictor variables to binary confidence
700 responses (low or high). In this framework, the sum of weighted predictor variables is
701 passed through a logistic link function which transforms the unbounded weighted sum
702 into the range of [0, 1]. The linear function is given by:

$$\gamma_i = \beta_0 + \beta_1 x_{i1} + \dots + \beta_U x_{iU} \quad (5)$$

703 where $x_{i1} \dots x_{iU}$ are the values for the U predictors on trial i , $\beta_1 \dots \beta_U$ are the weights
 704 for the respective predictors and β_0 is the intercept term. The inverse logistic link
 705 function that the linear function is passed through is given by:

$$c_i = \frac{\exp(\gamma)}{1 + \exp(\gamma)} \quad (6)$$

706 We used a multilevel extension of this model, such that we estimate the predictor
 707 weights, β s, for each subject. These weights are assumed to come from the same
 708 population such that the individual-subject β s are estimated concurrently with the
 709 mean and variance of the weights at the population level (Wallis et al., 2015). For the
 710 confidence model, we used a model with 9 predictor variables, where the linear
 711 function was described by:

$$\begin{aligned} h_i = & \beta_{j,0} + \beta_{j,1} \text{prior mismatch}_i + \beta_{j,2} \text{vertical energy}_i \\ & + \beta_{j,3} \text{horizontal energy}_i + \beta_{j,4} \text{oblique energy}_i \\ & + \beta_{j,5} |\text{phase}_i| + \beta_{j,6} \log(|\text{phase}_i|) + \beta_{j,7} \text{contrast}_i \\ & + \beta_{j,8} \text{rt}_i + \beta_{j,9} \text{experiment}_i \end{aligned} \quad (7)$$

712 such that for subject j , $\beta_{j,1} \dots \beta_{j,5}$ were the weights for the respective predictor variables
 713 and $\beta_{j,0}$ was the intercept. $\beta_{j,9}$ was the weight for an experiment indicator variable
 714 which allowed for differences in mean confidence across experiments (see
 715 **Supplementary Figure 1**). All predictors were standardised, by subtracting the mean
 716 and dividing by the standard deviation, prior to model fitting (see **Supplementary**
 717 **Figure 7**). The computation of each predictor variable is described below.

718 **Orientation Energy**

719 The goal of the confidence model was to determine if participants' confidence
 720 judgements were informed by the same prior used for their perceptual judgements.
 721 We reasoned that if participants used the same prior to inform their confidence, there
 722 would be a statistical association between confidence and the amount of
 723 correspondence in the distribution of low-level features in the target and the prior. To
 724 summarise the degree of overlap between the distribution of orientation features in the
 725 target and the prior, we used two sets of predictors: *prior mismatch* and *cardinal and*
 726 *oblique orientation energy*. For both sets of predictors, we assumed that participants
 727 use prior knowledge about the statistics of the distribution of orientation features in
 728 natural scenes to inform their confidence. For the prior mismatch predictor, we

729 assumed that observers directly compare a veridical representation of the distribution
730 of orientation energy in the stimulus and veridical knowledge of the prior distribution
731 of orientation energy to compute their confidence. This means that observers use a
732 statistic that summarises the mismatch between the *entire* distribution of orientation
733 energy in the target and the prior to compute their confidence. For the cardinal and
734 oblique orientation energy predictors, in contrast, we assume that observers rely on
735 only a *subset* of features in the stimulus and the prior model to compute their
736 confidence. Specifically, observers use a set of salient orientation cues, namely
737 vertical, horizontal, and oblique features, for confidence, based on prior knowledge
738 about the probability of these orientation features in the natural environment.

739 **Prior Mismatch.** For the prior mismatch predictor, we calculated the average
740 difference between the distribution of orientation energy in the target at the rotational
741 offset chosen by the participant and the prior distribution of orientation energy. We did
742 this by calculating the difference in orientation energy between the target and the prior
743 in each orientation bin, squaring this difference and then summing across bins.

744 **Cardinal and Oblique Orientation Energy.** For the cardinal and oblique
745 orientation energy predictors, we assumed that participants use a subset of orientation
746 features to estimate their confidence. We calculated orientation energy across all
747 orientations for each target positioned at the rotational offset chosen by the participant.
748 We then normalised energy for each orientation band so that each band expressed a
749 proportion of orientation energy in that bin relative to total orientation energy in the
750 target, a form of divisive normalisation (Carandini & Heeger, 2012; see
751 **Supplementary Figure 6**). To predict confidence, we use 3 predictors: *vertical energy*
752 (where $\theta = 90 \cdot \frac{\pi}{180}$), *horizontal energy* (where $\theta = 0$ or $180 \cdot \frac{\pi}{180}$), and *oblique energy*
753 (where $\theta = 45 \cdot \frac{\pi}{180}$ or $135 \cdot \frac{\pi}{180}$).

754 **Phase**

755 To summarise the degree of overlap between the phase in the target and the
756 prior, we used 2 *phase* predictors. For these predictors, we computed the response of
757 a broadscale filter positioned at the centre of the target with an orientation that
758 matched the rotational offset of the target. The response of the filter approximated the
759 strength of the horizon in the target and could be used to approximate the strength of
760 lighting in the scene (see **Figure 5C**). We used both the absolute value of the filter

761 response and a log transformation of the absolute value of the filter response as
762 predictors of confidence to allow for non-linear relationships between phase and
763 confidence.

764 **Response Time**

765 As described above, we also considered the possibility that confidence
766 depended on other heuristic cues not related to the prior. Based on previous research
767 (Faivre et al., 2018; Patel et al., 2012; van den Berg, Anandalingam, et al., 2016), we
768 therefore included a predictor in the confidence model for *response time*. For the
769 response time predictor, we used the response time of the orientation response for
770 each trial, measured in milliseconds.

771 **Contrast**

772 We also postulated that participants may use the contrast of the target as a
773 heuristic cue for confidence. For the *contrast* predictor, we used the root-mean-square
774 (RMS) contrast of each target (Bex & Makous, 2002; Harrison, 2022). RMS contrast
775 is the standard deviation of the luminance (i.e., pixel) values:

$$C_{rms} = \sqrt{\frac{1}{N-1} \sum_{k=1}^N (i_k - L)^2} \quad (8)$$

776 Where k is a pixel index, N is the total number of pixels, and L is the mean luminance.

777 **Summary of Modelling Approach**

778 To summarise our expectations about the confidence modelling results, we
779 reasoned that if participants used the perceptual prior to inform their confidence, we
780 would find that the measures which summarise the degree of overlap in orientation
781 energy between the target and the prior (prior mismatch and/or cardinal/oblique
782 orientation energy) and phase (absolute phase and/or log absolute phase) predicted
783 confidence. If, however, participants used other non-prior related measures to inform
784 their confidence, we would expect the other heuristic cues, such as the first order
785 response time or contrast, to be the only predictors of confidence.

References

- 786
787 Adams, W. J. (2007). A common light-prior for visual search, shape, and reflectance
788 judgments. *Journal of Vision*, 7(11), 11. <https://doi.org/10.1167/7.11.11>
- 789 Adler, W. T., & Ma, W. J. (2018). Comparing Bayesian and non-Bayesian accounts of
790 human confidence reports. *PLOS Computational Biology*, 14(11), e1006572.
791 <https://doi.org/10.1371/journal.pcbi.1006572>
- 792 Aitchison, L., Bang, D., Bahrami, B., & Latham, P. E. (2015). Doubly Bayesian Analysis
793 of Confidence in Perceptual Decision-Making. *PLOS Computational Biology*,
794 11(10), e1004519. <https://doi.org/10.1371/journal.pcbi.1004519>
- 795 A-Izzeddin, E. J., Mattingley, J. B., & Harrison, W. J. (2022). *Contextual influences of*
796 *visual perceptual inferences* [Preprint]. Neuroscience.
797 <https://doi.org/10.1101/2022.09.15.507892>
- 798 Appelle, S. (1972). Perception and discrimination as a function of stimulus orientation:
799 The “oblique effect” in man and animals. *Psychological Bulletin*, 78(4), 266–
800 278. <https://doi.org/10.1037/h0033117>
- 801 Beck, J. M., Ma, W. J., Kiani, R., Hanks, T., Churchland, A. K., Roitman, J., Shadlen,
802 M. N., Latham, P. E., & Pouget, A. (2008). Probabilistic Population Codes for
803 Bayesian Decision Making. *Neuron*, 60(6), 1142–1152.
804 <https://doi.org/10.1016/j.neuron.2008.09.021>
- 805 Berkley, M. A., Kitterle, F., & Watkins, D. W. (1975). Grating visibility as a function of
806 orientation and retinal eccentricity. *Vision Research*, 15(2), 239–244.
807 [https://doi.org/10.1016/0042-6989\(75\)90213-8](https://doi.org/10.1016/0042-6989(75)90213-8)
- 808 Bertana, A., Chetverikov, A., van Bergen, R. S., Ling, S., & Jehee, J. F. M. (2021).
809 Dual strategies in human confidence judgments. *Journal of Vision*, 21(5), 21.
810 <https://doi.org/10.1167/jov.21.5.21>

811 Bex, P. J., & Makous, W. (2002). Spatial frequency, phase, and the contrast of natural
812 images. *Journal of the Optical Society of America A*, 19(6), 1096.
813 <https://doi.org/10.1364/JOSAA.19.001096>

814 Boldt, A., de Gardelle, V., & Yeung, N. (2017). The impact of evidence reliability on
815 sensitivity and bias in decision confidence. *Journal of Experimental*
816 *Psychology: Human Perception and Performance*, 43(8), 1520–1531.
817 <https://doi.org/10.1037/xhp0000404>

818 Brainard, D. H. (1997). The Psychophysics Toolbox. *Spatial Vision*, 10(4), 433–436.
819 <https://doi.org/10.1163/156856897X00357>

820 Brewster, D. (1826). On the optical illusion of the conversion of cameos into intaglios,
821 and of intaglios into cameos with an account of other analogous phenomena.
822 *Edinburgh Journal of Science*, 4(7), 99–108.

823 Burge, J., & Geisler, W. S. (2011). Optimal defocus estimation in individual natural
824 images. *Proceedings of the National Academy of Sciences*, 108(40), 16849–
825 16854. <https://doi.org/10.1073/pnas.1108491108>

826 Campbell, F. W., Kulikowski, J. J., & Levinson, J. (1966). The effect of orientation on
827 the visual resolution of gratings. *The Journal of Physiology*, 187(2), 427–436.
828 <https://doi.org/10.1113/jphysiol.1966.sp008100>

829 Campbell, F. W., & Robson, J. G. (1968). Application of Fourier analysis to the visibility
830 of gratings. *The Journal of Physiology*, 197(3), 551–566.

831 Carandini, M., & Heeger, D. J. (2012). Normalization as a canonical neural
832 computation. *Nature Reviews Neuroscience*, 13(1), 51–62.
833 <https://doi.org/10.1038/nrn3136>

834 Dakin, S. C. (2001). Information limit on the spatial integration of local orientation
835 signals. *Journal of the Optical Society of America A*, 18(5), 1016.
836 <https://doi.org/10.1364/JOSAA.18.001016>

837 Dakin, S. C., & Watt, R. J. (1997). The computation of orientation statistics from visual
838 texture. *Vision Research*, 37(22), 3181–3192. <https://doi.org/10.1016/S0042->
839 [6989\(97\)00133-8](https://doi.org/10.1016/S0042-6989(97)00133-8)

840 de Gardelle, V., Kouider, S., & Sackur, J. (2010). An oblique illusion modulated by
841 visibility: Non-monotonic sensory integration in orientation processing. *Journal*
842 *of Vision*, 10(10), 6–6. <https://doi.org/10.1167/10.10.6>

843 Denison, R. N., Adler, W. T., Carrasco, M., & Ma, W. J. (2018). Humans incorporate
844 attention-dependent uncertainty into perceptual decisions and confidence.
845 *Proceedings of the National Academy of Sciences*, 115(43), 11090–11095.
846 <https://doi.org/10.1073/pnas.1717720115>

847 Desender, K., Boldt, A., & Yeung, N. (2018). Subjective Confidence Predicts
848 Information Seeking in Decision Making. *Psychological Science*, 29(5), 761–
849 778. <https://doi.org/10.1177/0956797617744771>

850 Faivre, N., Filevich, E., Solovey, G., Kühn, S., & Blanke, O. (2018). Behavioral,
851 Modeling, and Electrophysiological Evidence for Supramodality in Human
852 Metacognition. *Journal of Neuroscience*, 38(2), 263–277.
853 <https://doi.org/10.1523/JNEUROSCI.0322-17.2017>

854 Geisler, W. S., & Perry, J. S. (2011). Statistics for optimal point prediction in natural
855 images. *Journal of Vision*, 11(12), 14–14. <https://doi.org/10.1167/11.12.14>

856 Girshick, A. R., Landy, M. S., & Simoncelli, E. P. (2011). Cardinal rules: Visual
857 orientation perception reflects knowledge of environmental statistics. *Nature*
858 *Neuroscience*, 14(7), 926–932. <https://doi.org/10.1038/nn.2831>

859 Hangya, B., Sanders, J. I., & Kepecs, A. (2016). A Mathematical Framework for
860 Statistical Decision Confidence. *Neural Computation*, 28(9), 1840–1858.
861 https://doi.org/10.1162/NECO_a_00864

862 Hansen, B. C., & Essock, E. A. (2004). A horizontal bias in human visual processing
863 of orientation and its correspondence to the structural components of natural
864 scenes. *Journal of Vision*, 4(12), 5. <https://doi.org/10.1167/4.12.5>

865 Hansen, B. C., Essock, E. A., Zheng, Y., & Deford, J. K. (2003). Perceptual
866 anisotropies in visual processing and their relation to natural image statistics.
867 *Network: Computation in Neural Systems*, 14(3), 501–526.
868 https://doi.org/10.1088/0954-898X_14_3_307

869 Hansen, B. C., Haun, A. M., & Essock, E. A. (2008). The “Horizontal Effect”: A
870 perceptual anisotropy in visual processing of naturalistic broadband stimuli. In
871 T. A. Portocello & R. B. Velloti (Eds.), *Visual cortex: New research* (2nd ed.).
872 Nova Science Publishers.

873 Harrison, W. J. (2022). Luminance and Contrast of Images in the THINGS Database.
874 *Perception*, 51(4), 244–262. <https://doi.org/10.1177/03010066221083397>

875 Harrison, W. J., Bays, P. M., & Rideaux, R. (2023). *Neural tuning instantiates prior*
876 *expectations in the human visual system* (p. 2023.01.26.525790). bioRxiv.
877 <https://doi.org/10.1101/2023.01.26.525790>

878 Li, H.-H., & Ma, W. J. (2020). Confidence reports in decision-making with multiple
879 alternatives violate the Bayesian confidence hypothesis. *Nature*
880 *Communications*, 11(1), 2004. <https://doi.org/10.1038/s41467-020-15581-6>

881 Lisi, M., Mongillo, G., Milne, G., Dekker, T., & Gorea, A. (2021). Discrete confidence
882 levels revealed by sequential decisions. *Nature Human Behaviour*, 5(2), 273–
883 280. <https://doi.org/10.1038/s41562-020-00953-1>

884 Locke, S. M., Landy, M. S., & Mamassian, P. (2022). Suprathreshold perceptual
885 decisions constrain models of confidence. *PLOS Computational Biology*, *18*(7),
886 e1010318. <https://doi.org/10.1371/journal.pcbi.1010318>

887 Ma, W. J., Beck, J. M., Latham, P. E., & Pouget, A. (2006). Bayesian inference with
888 probabilistic population codes. *Nature Neuroscience*, *9*(11), 1432–1438.
889 <https://doi.org/10.1038/nn1790>

890 Ma, W. J., & Jazayeri, M. (2014). Neural Coding of Uncertainty and Probability. *Annual*
891 *Review of Neuroscience*, *37*(1), 205–220. [https://doi.org/10.1146/annurev-](https://doi.org/10.1146/annurev-neuro-071013-014017)
892 [neuro-071013-014017](https://doi.org/10.1146/annurev-neuro-071013-014017)

893 Metzger, W. (1936). *Gesetze des Sehens. [Laws of vision.]* (pp. xvi, 172). Kramer.

894 Michael, E., de Gardelle, V., Nevado-Holgado, A., & Summerfield, C. (2015).
895 Unreliable Evidence: 2 Sources of Uncertainty During Perceptual Choice.
896 *Cerebral Cortex*, *25*(4), 937–947. <https://doi.org/10.1093/cercor/bht287>

897 Mole, C. D., Jersakova, R., Kountouriotis, G. K., Moulin, C. J., & Wilkie, R. M. (2018).
898 Metacognitive judgements of perceptual-motor steering performance. *Quarterly*
899 *Journal of Experimental Psychology*, *71*(10), 2223–2234.
900 <https://doi.org/10.1177/1747021817737496>

901 Murray, R. F. (2013). The Statistics of Shape, Reflectance, and Lighting in Real-World
902 Scenes. In S. J. Dickinson & Z. Pizlo (Eds.), *Shape Perception in Human and*
903 *Computer Vision: An Interdisciplinary Perspective* (pp. 225–235). Springer
904 London. https://doi.org/10.1007/978-1-4471-5195-1_16

905 Navajas, J., Hindocha, C., Foda, H., Keramati, M., Latham, P. E., & Bahrami, B.
906 (2017). The idiosyncratic nature of confidence. *Nature Human Behaviour*,
907 *1*(11), 810–818. <https://doi.org/10.1038/s41562-017-0215-1>

908 Patel, D., Fleming, S. M., & Kilner, J. M. (2012). Inferring subjective states through the
909 observation of actions. *Proceedings of the Royal Society B: Biological*
910 *Sciences*, 279(1748), 4853–4860. <https://doi.org/10.1098/rspb.2012.1847>

911 Pelli, D. G. (1997). The VideoToolbox software for visual psychophysics: Transforming
912 numbers into movies. *Spatial Vision*, 10(4), 437–442.
913 <https://doi.org/10.1163/156856897X00366>

914 Pouget, A., Drugowitsch, J., & Kepecs, A. (2016). Confidence and certainty: Distinct
915 probabilistic quantities for different goals. *Nature Neuroscience*, 19(3), 366–
916 374. <https://doi.org/10.1038/nn.4240>

917 Pratte, M. S., Park, Y. E., Rademaker, R. L., & Tong, F. (2016). Accounting for
918 stimulus-specific variation in precision reveals a discrete capacity limit in visual
919 working memory. *Journal of Experimental Psychology: Human Perception and*
920 *Performance*, 43(1), 6–17. <https://doi.org/10.1037/xhp0000302>

921 Qamar, A. T., Cotton, R. J., George, R. G., Beck, J. M., Prezhdo, E., Laudano, A.,
922 Tolias, A. S., & Ma, W. J. (2013). Trial-to-trial, uncertainty-based adjustment of
923 decision boundaries in visual categorization. *Proceedings of the National*
924 *Academy of Sciences*, 110(50), 20332–20337.
925 <https://doi.org/10.1073/pnas.1219756110>

926 Ramachandran, V. S. (1988). *Perception of shape from shading*.

927 Rideaux, R., West, R. K., Wallis, T. S. A., Bex, P. J., Mattingley, J. B., & Harrison, W.
928 J. (2022a). Spatial structure, phase, and the contrast of natural images. *Journal*
929 *of Vision*, 22(1), 1–19. <https://doi.org/10.1167/jov.22.1.4>

930 Rideaux, R., West, R. K., Wallis, T. S. A., Bex, P. J., Mattingley, J. B., & Harrison, W.
931 J. (2022b). Spatial structure, phase, and the contrast of natural images. *Journal*
932 *of Vision*, 22(1), 4. <https://doi.org/10.1167/jov.22.1.4>

933 Sanders, J. I., Hangya, B., & Kepecs, A. (2016). Signatures of a Statistical
934 Computation in the Human Sense of Confidence. *Neuron*, *90*(3), 499–506.
935 <https://doi.org/10.1016/j.neuron.2016.03.025>

936 Spence, M. L., Dux, P. E., & Arnold, D. H. (2016). Computations underlying confidence
937 in visual perception. *Journal of Experimental Psychology: Human Perception*
938 *and Performance*, *42*(5), 671–682. <https://doi.org/10.1037/xhp0000179>

939 van den Berg, R., Anandalingam, K., Zylberberg, A., Kiani, R., Shadlen, M. N., &
940 Wolpert, D. M. (2016). A common mechanism underlies changes of mind about
941 decisions and confidence. *ELife*, *5*, e12192.
942 <https://doi.org/10.7554/eLife.12192>

943 van den Berg, R., Zylberberg, A., Kiani, R., Shadlen, M. N., & Wolpert, D. M. (2016).
944 Confidence Is the Bridge between Multi-stage Decisions. *Current Biology*,
945 *26*(23), 3157–3168. <https://doi.org/10.1016/j.cub.2016.10.021>

946 Wallis, T. S. A., Dorr, M., & Bex, P. J. (2015). Sensitivity to gaze-contingent contrast
947 increments in naturalistic movies: An exploratory report and model comparison.
948 *Journal of Vision*, *15*(8), 3. <https://doi.org/10.1167/15.8.3>

949 Wei, X.-X., & Stocker, A. A. (2015). A Bayesian observer model constrained by
950 efficient coding can explain “anti-Bayesian” percepts. *Nature Neuroscience*,
951 *18*(10), 1509–1517. <https://doi.org/10.1038/nn.4105>

952 West, R. K., Harrison, W. J., Matthews, N., Mattingley, J. B., & Sewell, D. K. (2022).
953 *Modality Independent or Modality Specific? Common Computations Underlie*
954 *Confidence Judgements in Visual and Auditory Decisions* [Preprint].
955 Neuroscience. <https://doi.org/10.1101/2022.10.31.514447>

956